ISSN 1009－3095 *Journal of Zhejiang University SCIENCE* V.4，No.1，P.1－7，Jan.－Feb.，2003
http://www.periodicals.com.cn；http://www.zju.edu.cn/English
http://www.zjupress.com；http://lib.zju.edu.cn/eindex.htm；jzu_s@mail.hz.zj.cn

Three-dimensional analysis of a thick FGM rectangular plate in thermal environment*

CHEN Wei-qiu(陈伟球)†，BIAN Zu-guang(边祖光)，DING Hao-jiang(丁皓江)
(*Department of Civil Engineering，Zhejiang University，Hangzhou 310027，China*)
†E-mail：chenwq@ccea.zju.edu.cn
Received Dec.26，2001；revision accepted Apr.20，2002

Abstract: The thermal behavior of a thick transversely isotropic FGM rectangular plate was investigated within the scope of three-dimensional elasticity. Noticing many FGMs may have temperature-dependent properties，the material constants were further considered as functions of temperature. A solution method based on state-space formulations with a laminate approximate model was proposed. For a thin plate，the method was clarified by comparison with the thin plate theory. The influences of material inhomogeneity and temperature-dependent characteristics were finally discussed through numerical examples.

Key words: Functionally graded material (FGM)，State-space method，Simply supported rectangular plate
Document code: A **CLC number:** O343.6；O343.8；TB39

INTRODUCTION

As known，thermal behaviors of structures must be considered in many situations. Study of thermal effect on deformations and stresses of a plate，especially a thick plate is increasingly important. First，the problems of thick plates are more complicated and thus more attractive to many scientists. Second，there are practical requirements for thick plates in various modern projects，such as high building，raceway，highway，container wharf，and so on. Many studies on thick and laminated plates had been reported (Wu and Tauchert，1980；Reddy，1997，1999). Xu et al. (1998) established a sixth-order，inhomogenous state equation for an orthotropic elastic body，and investigated the thermal response of an orthotropic thick laminated plate.

Functionally graded material (FGM) is in fact a special kind of inhomogeneous material with smoothly varying constitutive properties，responsible for its heat-resistant characteristics that can meet the needs of engineering construction materials. Therefore FGM is receiving considerably more attention in recent years (Chen et al.，2001，2002；Xu and Zhao，2001).

In thermal environment，the material constants of FGM are actually temperature-dependent and can be expressed as (Touloukian，1967)

$$M = C_0(C_{-1}t^{-1} + 1 + C_1 t + C_2 t^2 + C_3 t^3) \quad (1)$$

where t is Kelvin temperature and C_i are constants. Reddy and Chin (1998) used first-order shear plate theory to analyze the thermoelastic responses of an FGM plate using finite element method. Loy et al. (1999) employed Rayleigh-Ritz method to consider the vibration of FGM cylindrical shells from the viewpoint of Love's shell theory.

The thermal deformations and stresses of a thick transversely isotropic FGM rectangular plate in thermal environment were investigated in this work. Three-dimensional elasticity equations were used to derive a second-order homogenous state equation and a fourth-order inhomogenous state equation by introducing two displacement and two stress functions. The layerup model was used to approximate the FGM plate，which should be more and more accurate with the increasing number of layers. The material constants were assumed to be temperature-dependent as shown in Eq.(1). The analytical solution for a simply supported rectangular plate with arbitrary thickness-to-span ratio was obtained，and the

* Project (No.10002016) supported by National Natural Science Foundation of China

analytic solution for a thin plate was accorded well with thin plate theory. The influence of the material gradient index as well as that of temperature-dependent property on thermal behavior were discussed.

STATE-SPACE FORMULATIONS

In Cartesian coordinates (x, y, z), with $x-y$ plane identical with the isotropic plane of the material, the constitutive relations involving thermal effect of a transversely isotropic elastic body are (Ding et al., 2002)

$$\begin{aligned}
\sigma_x &= c_{11}\frac{\partial u}{\partial x} + c_{12}\frac{\partial v}{\partial y} + c_{13}\frac{\partial w}{\partial z} + \beta_1 T, \quad \tau_{yz} = c_{44}\left(\frac{\partial v}{\partial z} + \frac{\partial w}{\partial y}\right)\\
\sigma_y &= c_{12}\frac{\partial u}{\partial x} + c_{11}\frac{\partial v}{\partial y} + c_{13}\frac{\partial w}{\partial z} + \beta_1 T, \quad \tau_{xz} = c_{44}\left(\frac{\partial u}{\partial z} + \frac{\partial w}{\partial x}\right)\\
\sigma_z &= c_{13}\frac{\partial u}{\partial x} + c_{13}\frac{\partial v}{\partial y} + c_{33}\frac{\partial w}{\partial z} + \beta_3 T, \quad \tau_{xy} = c_{66}\left(\frac{\partial u}{\partial y} + \frac{\partial v}{\partial x}\right)
\end{aligned} \tag{2}$$

where σ_i and τ_{ij} are the normal and shear stress components respectively; u, v and w are the displacement components in x, y and z directions respectively; T is the excess temperature above the reference temperature t_0 in a stress-free state; c_{ij} are elastic constants and $c_{66}=(c_{11}-c_{12})/2$; β_1 and β_3 are thermal moduli defined by

$$\begin{aligned}
-\beta_1 &= c_{11}\alpha_1 + c_{12}\alpha_1 + c_{13}\alpha_3,\\
-\beta_3 &= c_{13}\alpha_1 + c_{13}\alpha_1 + c_{33}\alpha_3,
\end{aligned}$$

in which α_i are linear thermal expansion coefficients. Considering the material's graded property, we assume c_{ij} and α_i are functions of the coordinate z. In addition, to reflect the physical reality, all these constants shall be functions of the temperature $t(=t_0+T)$, as shown in Eq. (1).

In absence of body forces, the equations of equilibrium are

$$\begin{aligned}
\frac{\partial \sigma_x}{\partial x} + \frac{\partial \tau_{xy}}{\partial y} + \frac{\partial \tau_{xz}}{\partial z} &= 0\\
\frac{\partial \tau_{xy}}{\partial x} + \frac{\partial \sigma_y}{\partial y} + \frac{\partial \tau_{yz}}{\partial z} &= 0\\
\frac{\partial \tau_{xz}}{\partial x} + \frac{\partial \tau_{yz}}{\partial y} + \frac{\partial \sigma_z}{\partial z} &= 0
\end{aligned} \tag{3}$$

It can be shown that a sixth-order state equation for transversely isotropic thermoelasticity can be directly derived from the one for orthotropic thermoelasticity if certain constrained relations of elastic constants are introduced (Fan, 1996; Xu et al., 1998; Ding et al., 2002). Here, however, we apply the following substitutions (Chen, et al., 2001)

$$\begin{aligned}
u &= -\frac{\partial \psi}{\partial y} - \frac{\partial G}{\partial x}, \quad v = \frac{\partial \psi}{\partial x} - \frac{\partial G}{\partial y},\\
\tau_{xz} &= -\frac{\partial \tau_1}{\partial y} - \frac{\partial \tau_2}{\partial x}, \quad \tau_{yz} = \frac{\partial \tau_1}{\partial x} - \frac{\partial \tau_2}{\partial y}
\end{aligned} \tag{4}$$

where ψ and G are displacement functions, while τ_1 and τ_2 are stress functions. With Eq. (4), we can derive from Eqs. (2) and (3) after tedious mathematical manipulation:

$$\frac{\partial}{\partial z}\begin{Bmatrix}\psi\\ \tau_1\end{Bmatrix} = \begin{bmatrix}0 & 1/c_{44}\\ -c_{66}\Lambda & 0\end{bmatrix}\begin{Bmatrix}\psi\\ \tau_1\end{Bmatrix} \tag{5}$$

$$\frac{\partial}{\partial z}\begin{Bmatrix}G\\ \sigma_z\\ \tau_2\\ w\end{Bmatrix} = \begin{bmatrix}0 & 0 & 1/c_{44} & 1\\ 0 & 0 & \Lambda & 0\\ -(c_{11}-c_{13}^2/c_{33})\Lambda & c_{13}/c_{33} & 0 & 0\\ (c_{13}/c_{33})\Lambda & 1/c_{33} & 0 & 0\end{bmatrix}\begin{Bmatrix}G\\ \sigma_z\\ \tau_2\\ w\end{Bmatrix} + \begin{Bmatrix}0\\ 0\\ \dfrac{(c_{33}\beta_1 - c_{13}\beta_3)}{c_{33}}T\\ -\dfrac{\beta_3}{c_{33}}T\end{Bmatrix} \tag{6}$$

where $\Lambda = \partial^2/\partial x^2 + \partial^2/\partial y^2$. Although the total order of Eq. (5) and Eq. (6) is still six, the order of either single equation has been reduced, which is helpful for solving practical problems.

By virtue of Eq. (2), the other three stress components can be expressed in terms of state variables as

$$\sigma_x + \sigma_y = -\left(c_{11} + c_{12} - 2\frac{c_{13}^2}{c_{33}}\right)\Lambda G + 2\frac{c_{13}}{c_{33}}\sigma_z + 2\frac{(c_{33}\beta_1 - c_{13}\beta_3)}{c_{33}}T$$

$$\sigma_x - \sigma_y = -2c_{66}\left[2\frac{\partial^2\psi}{\partial x\partial y} + \left(\frac{\partial^2}{\partial x^2} - \frac{\partial^2}{\partial y^2}\right)G\right]$$

$$\tau_{xy} = c_{66}\left[\left(\frac{\partial^2}{\partial x^2} - \frac{\partial^2}{\partial y^2}\right)\psi - 2\frac{\partial^2 G}{\partial x\partial y}\right] \tag{7}$$

THERMAL ANALYSIS OF AN FGM RECTANGULAR PLATE

Consider a simply supported transversely isotropic FGM rectangular plate with the isotropic plate parallel to its middle plane. The geometry and coordinates of the plate are shown in Fig. 1. It is difficult to solve Eqs. (5) and (6) directly due to their variable coefficients matrices. Now we employ the laminate approximate model, in which we divide the plate into p equal layers. The thickness of each layer h/p is assumed to be very small, where h is the thickness of the plate.

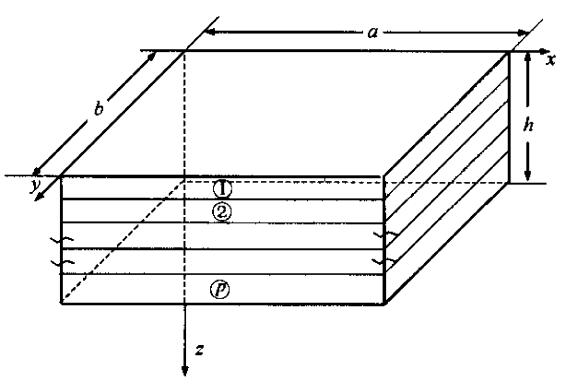

Fig.1 Plate geometry and Cartesian coordinates

Assume

$$\begin{bmatrix}\psi\\ \tau_1\end{bmatrix} = \sum_{m=0}^{\infty}\sum_{n=0}^{\infty}\begin{Bmatrix}h^2\bar{\psi}(\zeta)\\ hc_{44}^0\bar{\tau}_1(\zeta)\end{Bmatrix}\cos(m\pi\xi)\cos(n\pi\eta) \tag{8}$$

$$\begin{bmatrix}G\\ \sigma_z\\ \tau_2\\ w\end{bmatrix} = \sum_{m=1}^{\infty}\sum_{n=1}^{\infty}\begin{bmatrix}h^2\bar{G}(\zeta)/J_{mn}\\ c_{44}^0\bar{\sigma}_z(\zeta)\\ hc_{44}^0\bar{\tau}_2(\zeta)\\ h\bar{w}(\zeta)\end{bmatrix}\sin(m\pi\xi)\sin(n\pi\eta) \tag{9}$$

where $\zeta = z/h$, $\xi = x/a$ and $\eta = y/b$ are dimensionless coordinates; $J_{mn} = -(s_1^2 + s_2^2)$, $s_1 = (h/a)m\pi$, $s_2 = (h/b)n\pi$; c_{44}^0 represents the value of c_{44} at $z = 0$, etc. It is immediately seen that the solutions given in Eqs. (8) and (9) satisfy the simply supported conditions in the three-dimensional sense (Fan, 1996; Ding et al., 2002). At the same time, we expand the arbitrary temperature difference T as given below:

$$T(\xi,\eta,\zeta) = \sum_{m=1}^{\infty}\sum_{n=1}^{\infty}\bar{T}(\zeta)\sin(m\pi\xi)\sin(n\pi\eta) \tag{10}$$

where $\bar{T}(\zeta) = 4\int_0^1\int_0^1 T(\xi,\eta,\zeta)\sin(m\pi\xi)\sin(n\pi\eta)\mathrm{d}\xi\mathrm{d}\eta$. Substituting Eqs. (8), (9) and (10) into Eqs. (5) and (6), and utilizing the orthogonal properties of trigonometric functions, one can obtain for an arbitrary couple of (m, n)

$$\frac{\mathrm{d}}{\mathrm{d}\zeta}\boldsymbol{V}_k(\zeta) = \boldsymbol{M}_k\boldsymbol{V}_k(\zeta) + \bar{T}(\zeta)\boldsymbol{H}_k \quad (k = 1,2) \tag{11}$$

where $\boldsymbol{V}_1 = [\bar{\psi}, \bar{\tau}_1]^{\mathrm{T}}$, $\boldsymbol{V}_2 = [\bar{G}, \bar{\sigma}_z, \bar{\tau}_2, \bar{w}]^{\mathrm{T}}$, $\boldsymbol{H}_1 = [0, 0]^{\mathrm{T}}$, $\boldsymbol{H}_2 = \left[0, 0, \frac{(c_{33}\beta_1 - c_{13}\beta_3)}{c_{33}c_{44}^0}, -\frac{\beta_3}{c_{33}}\right]^{\mathrm{T}}$, and

$$\boldsymbol{M}_1 = \begin{bmatrix}0 & \frac{c_{44}^0}{c_{44}}\\ -\frac{c_{66}J_{mn}}{c_{44}^0} & 0\end{bmatrix}$$

$$\boldsymbol{M}_2 = \begin{bmatrix}0 & 0 & \frac{c_{44}^0}{c_{44}}J_{mn} & J_{mn}\\ 0 & 0 & J_{mn} & 0\\ \frac{c_{13}^2 - c_{11}c_{33}}{c_{33}c_{44}^0} & \frac{c_{13}}{c_{33}} & 0 & 0\\ \frac{c_{13}}{c_{33}} & \frac{c_{44}^0}{c_{33}} & 0 & 0\end{bmatrix}$$

Since each layer is sufficiently thin, the material constants within it can be assumed constant rather than variable. In the following, their values at each mid-plane are to be taken, i.e. in Eq. (11), we have $c_{44} = c_{44}|_{\zeta = \frac{(2j-1)}{2p}}$ etc. in the j-th layer. Thus the coefficient matrices and column vectors in Eq. (11) become constant within any layer and the solutions can be obtained (Fan, 1996)

$$\boldsymbol{V}_k(\zeta)=\exp[(\zeta-\zeta_j)\boldsymbol{M}_k]\boldsymbol{V}_k(\zeta_j)+\boldsymbol{P}_k(\zeta)\boldsymbol{H}_k \quad \left(\frac{j-1}{p}=\zeta_j\leqslant\zeta\leqslant\frac{j}{p},\ j=1,2,\cdots,p\right) \tag{12}$$

where

$$\boldsymbol{P}_k(\zeta)=\int_{\zeta_j}^{\zeta}\exp[(\zeta-\tau)\boldsymbol{M}_k]\bar{T}(\tau)\mathrm{d}\tau \tag{13}$$

The exponential matrices $\exp[(\zeta-\zeta_j)\boldsymbol{M}_k]$ in Eq. (12) are known as the transfer matrices, which can be expressed as the polynomials of $\boldsymbol{M}_k$ if Cayley-Hamilton theorem is employed (Bellman, 1970).

The continuity conditions at each hypothetical interface $\zeta=j/p$ require that the six state variables be continuous. Thus one can obtain from Eq.(12)

$$\boldsymbol{V}_k(1)=\boldsymbol{T}_k\boldsymbol{V}_k(0)+\boldsymbol{S}_k \tag{14}$$

where $\boldsymbol{T}_k=\prod_{j=p}^{1}\exp(\boldsymbol{M}_k/p)$ are square matrices, and

$$\boldsymbol{S}_1=[0,0]^{\mathrm{T}},\quad \boldsymbol{S}_2=\sum_{i=p}^{1}\left[\prod_{j=p}^{i+1}\exp(\boldsymbol{M}_2/p)\right]\boldsymbol{C}_i \tag{15}$$

where $\boldsymbol{C}_i=\boldsymbol{P}_2(i/p)\cdot\boldsymbol{H}_2$, $\prod_{j=p}^{p+1}\exp(\boldsymbol{M}_2/p)=\boldsymbol{I}$. $\boldsymbol{I}$ is an identity. It is convenient and efficient to program using this form of $\boldsymbol{S}_2$.

It is assumed that the top and bottom surfaces of the plate are tractions free and hence the plate is only subjected to a temperature load. It can be shown that the state variables $\bar{\psi}$ and $\bar{\tau}_1$ vanish everywhere in the plate, and

$$\begin{Bmatrix}\bar{G}(1)\\0\\0\\\bar{w}(1)\end{Bmatrix}=\boldsymbol{T}_2\begin{Bmatrix}\bar{G}(0)\\0\\0\\\bar{w}(0)\end{Bmatrix}+\boldsymbol{S}_2 \tag{16}$$

which gives

$$\begin{Bmatrix}\bar{G}(0)\\\bar{w}(0)\end{Bmatrix}=-\begin{bmatrix}T_{221}&T_{224}\\T_{231}&T_{234}\end{bmatrix}^{-1}\begin{Bmatrix}S_{22}\\S_{23}\end{Bmatrix} \tag{17}$$

where T_{2ij} are elements of the matrix $\boldsymbol{T}_2$, S_{2i} are elements of the column vector $\boldsymbol{S}_2$. Once the state variables at the top surface are known, the nonzero state variables at an arbitrary interior point can be obtained by Eq. (12) and the induced variables are determined from Eq. (7).

The above analysis can be applied to an isotropic plate if the following relations $c_{11}=c_{33}=\lambda+2\mu$, $c_{12}=c_{13}=\lambda$, $c_{44}=\mu$ and $\alpha_1=\alpha_3$ are introduced, here λ and μ are two Lame constants (Ding et al., 2002).

NUMERICAL EXAMPLES

For numerical investigation, an excess temperature distribution $T=\bar{T}(\zeta)\sin(\pi\xi)\sin(\pi\eta)$, with $\bar{T}(\zeta)=(\bar{T}_1-\bar{T}_0)\cdot\zeta+\bar{T}_0$ is considered. It is obvious that $\bar{T}_0$ and $\bar{T}_1$ are the excess temperatures at the central points on the top and bottom surfaces, respectively.

The functionally graded property of the material is represented by (Reddy et al., 1999)

$$M(t,z)=M_I(t)\left(\frac{h-z}{h}\right)^{\kappa}+M_{II}(t)\left[1-\left(\frac{h-z}{h}\right)^{\kappa}\right] \tag{18}$$

where $M(t, z)$ represents an arbitrary material constant of FGM, while $M_I(t)$ and $M_{II}(t)$ are the corresponding ones for two homogenous materials. The dependency of $M_i(t)(i=I, II)$ on the temperature $t=t_0+T$ is shown in Eq. (1). For numerical calculation, $t_0=300\mathrm{K}$ is taken hereafter and $C_n(n=-1,\cdots,3)$ are listed in Table 1 for the two materials. The parameter κ in Eq. (18) is the gradient index. Obviously, the plate will be made of Material I only if $\kappa=0$.

First we consider a simply supported thin FGM rectangular plate with $a/h=40$ and $b/h=30$. It is easy to extend the thin plate theory (TPT) for isotropic homogeneous materials (Timoshenko and Woinowsky-Krieger, 1959) to transversely isotropic functionally graded materials. Results show that it is sufficiently accurate if the plate is divided into 30 layers when $\kappa=20$ and $\Delta T=\bar{T}_0-\bar{T}_1$ is not very large.

From Tables 2 and 3, we can find the two methods agree with each other very well. The displacements obtained by the thin plate theory are in-between the ones of the top and middle surfaces obtained by the present method.

Second, we consider a simply supported thick FGM rectangular plate with $a/h=4$ and $b/h=6$. $\bar{T}_1=5\mathrm{K}$ and $\Delta T=50\mathrm{K}$ are taken. Table 4 gives the nondimensional results when $p=30$ and $p=32$ (gradient index $\kappa=20$). It is shown that the relative errors between $p=30$ and $p=32$ meet the requirement of engineering (the biggest relative error is 0.94%). We will take $p=30$ in the following and the results are believed to be of high precision. It should be noted that the stresses σ_x and σ_y are not continuous across the hypothetical interface because of the laminate approximation. However, the distinction can be completely neglected within the significant digits.

Figs.2 and 3 display curves of the nondimensional displacement w/h and the nondimensional normal stress σ_x/c_{44}^0 at the central point of the middle surface versus the gradient index κ. The dotted lines correspond to the case when the

Table 1 Temperature-dependent coefficients of elastic constants c_{ij} (Pa) and linear thermal expansions α_i (1/K)

	Material I					Material II				
	C_{-1}	C_0	C_1	C_2	C_3	C_{-1}	C_0	C_1	C_2	C_3
c_{11}	0	2.084e11	−1.020e−3	0.160e−7	−1.995e−10	0	2.062e11	3.102e−4	−6.942e−7	0
c_{12}	0	1.191e11	−1.107e−3	0.541e−7	−1.535e−10	0	1.211e11	2.728e−4	−7.823e−7	0
c_{13}	0	6.309e10	−2.407e−3	0.339e−7	−1.815e−10	0	1.038e11	3.314e−4	−8.241e−7	0
c_{33}	0	3.667e11	−3.226e−4	3.339e−7	−1.009e−10	0	2.103e11	2.886e−4	−7.994e−7	0
c_{44}	0	2.096e11	−6.856e−4	1.624e−7	−9.385e−11	0	5.012e10	0.534e−4	−9.861e−7	0
α_1	0	1.101e−5	−2.841e−4	0	0	0	8.914e−6	−3.871e−4	0	0
α_3	0	5.714e−6	−4.416e−4	0	0	0	4.107e−6	−2.114e−4	0	0

Table 2 Central deflection w/h ($\times 10^{-3}$) for different temperatures ($\bar{T}_1=5$K, $\kappa=0$)

ΔT	Present			TPT	Relative errors (with middle plane)
	Top surface	Middle plane	Bottom surface		
5K	−5.451	−5.421	−5.400	−5.428	0.129%
30K	−32.816	−32.724	−32.681	−32.763	0.119%
50K	−54.937	−54.794	−54.735	−54.855	0.111%

Table 3 Central deflection w/h ($\times 10^{-3}$) for different temperatures ($\bar{T}_1=5$K, $\kappa=20$)

ΔT	Present			TPT	Relative errors (with middle plane)
	Top surface	Middle plane	Bottom surface		
5K	−4.939	−4.909	−4.886	−4.921	0.244%
30K	−27.876	−27.781	−27.736	−27.833	0.187%
50K	−46.457	−46.310	−46.246	−46.381	0.153%

Table 4 Comparison of various variables ($\times 10^{-3}$) for different layer-ups ($\kappa=20$)

Location	w/h		σ_x/c_{44}^0		σ_y/c_{44}^0		σ_z/c_{44}^0	
	$p=30$	$p=32$	$p=30$	$p=32$	$p=30$	$p=32$	$p=30$	$p=32$
Top surface	−1.033	−1.033	−0.211	−0.213	−0.345	−0.346	0.000	0.000
Middle surface	−0.886	−0.886	−0.381	−0.383	−0.471	−0.473	0.000	0.000
Bottom surface	−0.823	−0.823	−0.667	−0.668	−0.681	−0.682	0.001	0.001

material constants are taken unaltered and that the values at the initial stress-free temperature $t_0 = 300\text{K}$ are used. The curve of σ_y / c_{44}^0 is very similar to that of σ_x / c_{44}^0 and hence is not given here. From the figures, we can find that the gradient index κ has significant effect on the stress and deformation.

We now study further the influence of temperature-dependent property. A thick FGM plate as above described, but with $\bar{T}_1 = 100\text{K}$, is considered. It is shown that $p = 100$ is enough for an accurate result. Figs. 4 and 5 give the variations of w/h, the nondimentional displacement at the center on the middle plate, with ΔT for two values $\kappa = 0$ and 0.25, respectively. As shown above, the dotted lines are for the case of temperature-independent material constants with the values at $t_0 = 300\text{K}$. It is clearly shown that the material's temperature-dependent characteristic has important effect on the plate deformation.

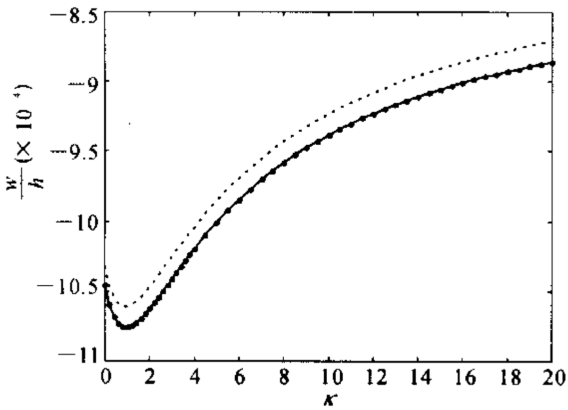

Fig.2 Variation of w/h at the center on middle surface with gradient index κ

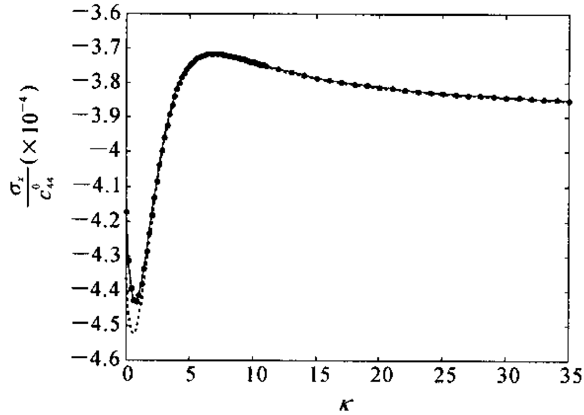

Fig.3 Variation of σ_x / c_{44}^0 at the center on middle surface with gradient index κ

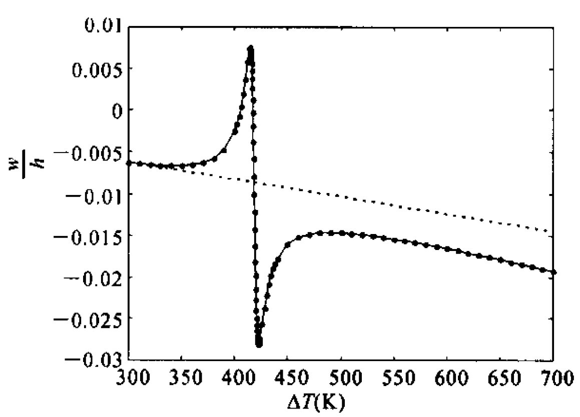

Fig.4 Variation of w/h at the center on middle surface with ΔT ($\kappa = 0$)

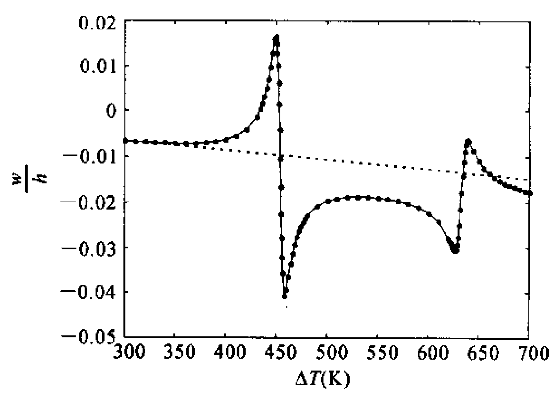

Fig.5 Variation of w/h at the center on middle surface with ΔT ($\kappa = 0.25$)

CONCLUSIONS

1. Using the state-space formulations, in connection with the laminate approximate model, the order of the final solving equations of an FGM plate does not vary with the number of the layers divided. It thus can improve the numerical efficiency as well as the numerical precision.

2. It is seen that for a thin FGM plate the thin plate theory agrees well with the present 3D analysis. The relative error between them decrease with the increase of ΔT. That is because

for a big ΔT, the bending deformation will prevail in the plate, which coincides with the basic assumption adopted in the thin plate theory.

3. Table 4 shows that the deflections of the plate in different locations along the thickness direction are quite different, which indicates that both the thin plate theory and the first-order shear plate theory are no longer suitable for thick FGM plate. On the other hand, the present analysis is valid for any thickness-to-span ratio and can be a benchmark of two-dimensional approximate plate theories or numerical methods.

4. Figs. 2 and 3 indicate that the material gradient index has significantly important effect on the thermal stresses and displacements, of which the sensitive ranges are not the same. This character can be used in engineering projects to meet some special requirements. Also, Figs. 4 and 5 show that the dependency of material properties on temperature will change the results to a considerable degree as ΔT increases. Thus in a severe thermal environment, such a dependency must be considered to accurate analysis results.

References

Bellman, R., 1970. Introduction to Matrix Analysis. McGraw-Hill, New York.

Chen, W. Q., Ye, G. R., Cai, J. B. and Ding, H. J., 2001. Free vibration of transversely isotropic FGM rectangular plates. *Journal of Vibration Engineering*, **14**(3): 263 – 267 (in Chinese).

Chen, W. Q., Ye, G. R. and Cai, J. B., 2002. Thermoelastic stresses in a uniformly heated functionally graded isotropic hollow cylinder. *Journal of Zhejiang University SCIENCE*, **3**(1): 1 – 5.

Ding, H. J., Zhang, L. C. and Chen, W. Q., 2002. Elasticity of Transversely Isotropic Materials. Trans Tech Publication, Zuerich.

Fan, J. R., 1996. Exact Theory of Strongly Thick Laminated Plates and Shells. Science Press, Beijing (in Chinese).

Loy, C. T., Lam, K. Y. and Reddy, J.N., 1999. Vibration of functionally graded cylindrical shells. *International Journal of Mechanical Sciences*, **41**(3): 309 – 324.

Reddy, J. N., 1997. Mechanics of Laminated Composite Plates, Theory and Analysis. CRC Press, Boca Raton.

Reddy, J. N., 1999. Theory and Analysis of Elastic Plates. Taylor & Francis, Philadelphia.

Reddy, J. N. and Chin, K., 1998. Thermomechanical behavior of functionally graded cylinders and plates. *Journal of Thermal Stresses*, **21**(3): 593 – 626.

Reddy, J. N., Wang, C. M. and Kitipornchai, S., 1999. Axisymmetric bending of functionally graded circular and annular plates. *European Journal of Mechanics A/Solids*, **18**(2): 185 – 199.

Timoshenko, S. P. and Woinowsky-Krieger, S., 1959. Theory of Plates and Shells. McGraw-Hill, New York.

Touloukian, Y. S., 1967. Thermophysical Properties of High Temperature Solid Materials. McMillan, New York.

Wu, C. H. and Tauchert, T. R., 1980. Thermoelastic analysis of laminated plates I: symmetric specially orthotropic laminates. *Journal of Thermal Stresses*, **3**(2): 247 – 259.

Xu, F., Xu, X. M. and Wang, Y. C., 1998. Research for the thermoelastic response of thick orthotropic laminates. *Chinese Journal of Computational Mechanics*, **15**(3): 306 – 315 (in Chinese).

Xu, Y., J. and Zhao, Z. G., 2001. Transient thermal bending analysis of thin plates of functionally gradient material by finite element method. *Engineering Mechanics*, **18**(1): 71 – 81 (in Chinese).